Design and development of model for proton exchange membrane fuel cell

Ankush Babaji Aher[1], Sudhir Madhav Patil[1], Tole Sutikno[2,3]

[1]Department of Manufacturing Engineering and Industrial Management, COEP Technological University (COEP Tech), Pune, India
[2]Master Program of Electrical Engineering, Faculty of Industrial Technology, Universitas Ahmad Dahlan, Yogyakarta, Indonesia
[3]Embedded Systems and Power Electronics Research Group, Yogyakarta, Indonesia

Article Info

ABSTRACT

Fuel prices are rising, and fossil fuel resources are depleting. This fuel is consumed by conventional fuel vehicles, which contributes to increased greenhouse gas emissions and air pollution. Various vehicle technologies have been introduced in modern times. Among these innovations, fuel cell vehicle technology stands out due to its ease of use, robustness, and simplicity. The primary energy source for this system is hydrogen. Fuel cells use hydrogen to generate electricity through a chemical process that does not involve combustion. The purpose of this paper is to describe the design and development of a simulation model for a fuel cell (proton exchange membrane type) vehicle using mathematical equations and the MATLAB/Simulink R2020a software, taking into account all voltage losses and temperature variations of the proton exchange membrane (PEM) type fuel cell. The designed model is validated in two ways: first by generating V-I characteristics for the designed PEM-type fuel cell, and then by performing a performance test in Simulink using the driving cycle on one of the fuel cell vehicles. The obtained simulated results are nearly identical to the expected results, and the designed PEM-type fuel cell performed well in all real-time driving cycle test conditions.

Corresponding Author:

Sudhir Madhav Patil
Department of Manufacturing Engineering and Industrial Management
COEP Technological University (COEP Tech)
Wellesley Road, Chhatrapati Shivajinagar, Pune-411005, Maharashtra State, India
Email: smp.prod@coeptech.ac.in, smp.mfg@coeptech.ac.in, sudhir.smp@gmail.com

1. INTRODUCTION

The Indian government is actively implementing stricter emission regulations to address the problem of vehicle pollution. Fuel price increases and the depletion of fossil fuel resources highlight the need for new technological advances in the automotive industry. Adoption of fuel cell hybrid vehicles (FCHVs) is one suggested solution to this problem.

The burning of fossil fuels is the primary contributor to both localized air pollution and global warming. The transportation and automobile sectors are the largest consumers of fossil fuels; as a result, the primary objective is to reduce and eliminate pollution from the transportation and automobile sectors [1]. Vehicle manufacturers are competing against one another to produce environmentally friendly automobiles because this is a current necessity. Now that electric vehicles are available on the market, however, consumers should be aware that these automobiles have several drawbacks, including a short driving range, a lengthy amount of time required to recharge the battery, and inefficient operation. These drawbacks of electric vehicles

can be circumvented by using a fuel cell hybrid vehicle (FCHV), which operates on batteries and fuel cells that use hydrogen as a fuel [2], [3].

Researchers have conducted experiments on a wide variety of fuel cell designs. One of the potential candidates is a fuel cell of the proton exchange membrane (PEM) variety. The electrolyte that is used in a fuel cell is typically used to differentiate between the various types of fuel cells; however, there are always other significant factors to consider. The investigation of the mathematical modeling of PEM-type fuel cells using MATLAB/Simulink is beneficial because of its broad applicability, potential for efficiency improvement, and environmental advantages. When selecting a fuel cell technology, however, researchers and engineers should be aware of the cost and durability challenges associated with PEM-type fuel cells and should take into consideration the particular application and context [4], [5].

PEM-type fuel cells are most suitable for vehicle applications because they allow for rapid start-up thanks to their low operating temperature. Internal-combustion engines find these to be an attractive choice because of their high-power density and robust mechanical structure [1], [4], [6]. The objective of this study is to create and construct a simulation model for proton exchange membrane (PEM) fuel cells specifically designed for use in vehicles, particularly four-wheeled vehicles. The model is formulated using mathematical equations through the utilization of MATLAB/Simulink software. This software aids in testing and assessing the feasibility of the output power in accordance with the specified requirements. This will also aid in comprehending the distinct operational zones of PEM-type fuel cells and identifying the optimal zone for PEM-type fuel cells to function in relation to voltage and current. Creating a MATLAB/Simulink model for a proton exchange membrane (PEM) fuel cell is a flexible and highly valuable tool. It has versatile applications, such as enhancing performance, analyzing systems, developing controls, conducting research, and facilitating education in the domain of fuel cell technology.

2. METHOD
2.1. Proton exchange membrane (PEM) fuel cell

A PEM-type fuel cell is made up of two electrodes: a negative-polarity anode and a positive-polarity cathode, as well as a membrane of solid electrolyte between them. It is the same as an electrochemical cell. Oxidization of hydrogen is on the anode side, while reduction of oxygen is on the cathode side. Anode-to-cathode proton transmission happens through the membrane of a solid electrolyte. Electrons flow to the cathode over an external circuit. On the cathode side, water and heat are generated as byproducts of a combined reaction between O_2, electrons, and protons. The electro-chemical reaction is accelerated due to the presence of a catalytic member on the anode as well as the cathode [7], [8]. A typical PEM-type fuel cell has the following reactions [7]:

− Anode: $H_2(g) \rightarrow 2H^+(aq) + 2e^-$
− Cathode: $\frac{1}{2}O_2(g) + 2H^+(aq) + 2e^- \rightarrow H_2O(l)$
− Overall: $H_2(g) + \frac{1}{2}O_2(g) \rightarrow H_2O(l)$ + electrical energy + thermal energy (heat as a by-product)

The fuel source for PEM fuel cells used in automotive applications is hydrogen gas. Figure 1 [9] shows how a fuel cell of the PEM type operates. The diagram shows that air is supplied to the cathode side and hydrogen gas passes through the anode side. The electrolyte in the fuel cell divides hydrogen into protons and electrons. Electrons follow an external circuit to create an electric current, while protons travel through the electrolyte to reach the cathode side. Heat and water are produced on the cathode side when oxygen, protons, and electrons mix. PEM-type fuel cells are suitable for automotive applications as they operate at low temperatures and give quick responses by varying output current and voltage to meet power requirements in vehicles as per load conditions.

2.2. Mathematical modelling of PEM type fuel cell

To model the fuel cell, the first step required is to calculate Nernst voltage of fuel cell and it is given by (1) [10]:

$$E_n = E_0 + (T - T_0)\frac{\Delta S}{zF} - \frac{RT}{zF}\ln(PH_2\sqrt{PO_2}) \tag{1}$$

where, E_n= fuel cell's Nernst voltage; E_0= standard-state reversible voltage; T = temperature of fuel cell in K; T_0 = room temperature in K; ΔS = change in entropy for H_2-O_2 fuel cell; z = no. of electrons that were transported during the process; F = Faraday's constant = 96485 $Cmol^{-1}$; R= gas constant =8.314 J $(molK)^{-1}$; PH_2 = partial pressure of hydrogen inside the stack; PO_2 = partial pressure of oxygen inside the stack.

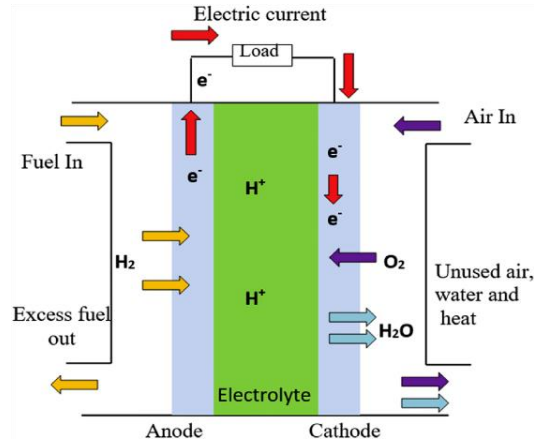Figure 1. Working of a PEM type fuel cell [9]

2.3. Identification of the Nernst voltage equation's key elements

A number of crucial factors need to be considered in order to calculate the Nernst voltage. Since hydrogen-oxygen fuel cells are our main area of interest, the following parameters are calculated specifically for this setting. A hydrogen–oxygen type fuel cell generates the standard-state reversible voltage (E_0) and is determined using (2) [10].

$$E_0 = -\frac{\Delta g°}{zF} \tag{2}$$

Where Δg = standard-state free energy change for the hydrogen-oxygen reaction; Δg = –237000 J mol^{-1}; $z = 2$, for hydrogen-oxygen fuel cell. Substituting all the known values, in (2).

$$E_0 = -\frac{-237000}{2 \times 96485}$$

$$E_0 = +1.229 \text{ V}$$

For an H_2-O_2 fuel cell operating in standard state conditions, the change in entropy (ΔS) is found to be –44.34 J (mol K)$^{-1}$, where (T_0) is the room temperature, which is 298 K. The partial pressure of oxygen (PO_2) and hydrogen (PH_2) depend on the vehicle's power requirement and reactant consumption. In the end, (3) represents the Nernst voltage equation for a hydrogen-oxygen fuel cell.

$$E_n = 1.229 - 2.298 \times 10^{-4} (T - 298) - \frac{RT}{zF} \ln(PH_2 \sqrt{PO_2}) \tag{3}$$

2.4. Fuel cell voltage

Voltage of one fuel cell and stack is determined by (4) and (5) respectively [11], [12]:

$$V_{\text{cell}} = E_n - V_{\text{act,cell}} - V_{\text{ohmic,cell}} - V_{\text{conc,cell}} \tag{4}$$

$$V_{\text{stack}} = N \times V_{\text{cell}} \tag{5}$$

where, V_{cell} = Voltage o/p of one fuel cell; $V_{\text{act,cell}}$ = activation loss of one fuel cell; $V_{\text{ohmic,cell}}$ = ohmic loss of one fuel cell; $V_{\text{conc,cell}}$ = concentration loss of single fuel cell; V_{stack} = fuel cell stack voltage; N = Number of cells in stack. The number of cells, required to obtain the anticipated output power, is computed using (6).

$$N = \frac{Voltage\ output\ required}{Voltage\ output\ of\ single\ fuel\ cell} \tag{6}$$

2.5. Voltage losses in PEM type fuel cell

Due to irreversible losses, the present fuel cell's voltage output is observed as lower than that estimated by thermodynamics principles. As shown in Figure 2, the following are three significant forms of fuel cell losses: in early part of curve, the electro-chemical process causes activation losses.
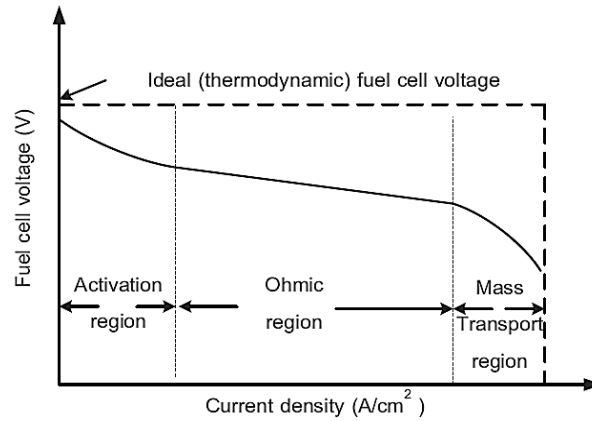
Figure 2. PEM type fuel cell voltage variation with net current density [11]

The ionic electronic state causes ohmic losses, in the central part of curve. Mass transfer causes concentration losses in the end of V-I curve [11].

a)   Activation loss: the phenomenon known as activation loss is the slow rate at which reactions take place on the electrode surfaces. As a result, some of the voltage produced is highly nonlinearly dissipated in order to support the chemical reactions that carry out the electron transfer to and from the electrode. The activation loss of fuel cell is given by (7) [4], [13]. The 'Tafel equation' is the name given to (7). The (8) helps to determine the Tafel slope.

$$V_{act} = A \times \ln(\frac{i}{i_0}) \tag{7}$$

$$A = \frac{RT}{2\alpha F} \tag{8}$$

Where, A = Tafel slope (V); I = current density (Ampere cm^{-2}); i_0 = exchange current density (ampere cm^{-2}); α = charge transfer coefficient in the range 0 to 1.0.

b)   Ohmic loss: the electrodes' electrical resistance is the cause of ohmic losses. The movement of ions in the electrolyte is hindered by a variety of connections and resistances. There is a linear relationship between the current density and the magnitude of the voltage drop. The ohmic loss of fuel cell is given by (9) [4], [12].

$$V_{ohm} = I \times R_{ohm} = I \times (R_{electronic} + R_{ionic}) \tag{9}$$

Where, I = fuel cell current (ampere); R_{ohm} = ohmic resistance (ohm 'Ω'); $R_{electronic}$ = resistance to the electron transport in electron conductive part (ohm 'Ω'); R_{ionic} = resistance to the flow of ions (ohm 'Ω').

c)   Concentration loss: concentration gradients are created during the reaction process as a result of the mass diffusion of reactants from the flow channels to the reaction sites, which causes concentration loss. The slow transport of reactants to the reaction sites causes concentration voltages to drop at high current densities, resulting in a non-linear voltage drop. The concentration loss of fuel cell is given by (10) [4], [14].

$$V_{conc} = \frac{RT}{2F} \ln(1 - \frac{I}{I_L}) \tag{10}$$

Where I_L = limiting current of fuel cell (ampere).

2.6. Thermodynamic energy balance

The net heat generated inside the PEM type fuel cell due to chemical reaction causes its temperature to increase or decrease. This net heat generation given by (11) [15].

$$q_{net} = q_{chem} - q_{elec} - q_{sens+latent} - q_{loss} \tag{11}$$

Where, q_{net} = net heat generated inside the PEM type fuel cell; q_{chem} = chemical energy generated inside the PEM type fuel cell; q_{elec} = electrical energy generated inside the fuel cell; $q_{sens+latent}$ = the sensible and latent heat generated inside the fuel cell; q_{loss} = heat loss due to convection inside the fuel cell.

2.7. Designed PEM type fuel cell

A PEM-type fuel cell is designed, modeled, and simulated using MATLAB/Simulink software. The designed fuel cell is modeled with the help of mathematical equations. The advantage and uniqueness of this designed PEM-type fuel cell model is that it consists of all PEM-type fuel cell voltage losses along with thermodynamic energy balance. As shown in Figure 3, the MATLAB model has mainly three subsystems. Nernst voltage and rate of utilization are calculated in one subsystem. In another second subsystem, all voltage losses are calculated for a single fuel cell, and then losses across the fuel cell stack are calculated by considering the number of cells. In the third thermodynamic energy balance subsystem, the temperature of the fuel cell is calculated. Voltage losses block as depicted in more detail in Figure 4 gives the activation voltage drop, ohmic voltage drop, and concentration voltage drop of a single cell. Figure 5 depicts the detailed simulation block pertaining to determination of rate of utilization of reactant and oxidant i.e., H_2, O_2 and O_2H_2. Other inputs required to calculate Nernst voltage are anode and cathode side supply pressure, and the composition of hydrogen and oxygen. Figure 6 depicts that Tafel slope, exchange current density and change in enthalpy are also calculated along with Nernst voltage. Figure 7 depicts the thermodynamic energy balance subsystem. This subsystem helps to calculate net heat generated inside the fuel cell, and further helps to determine temperature of fuel cell.
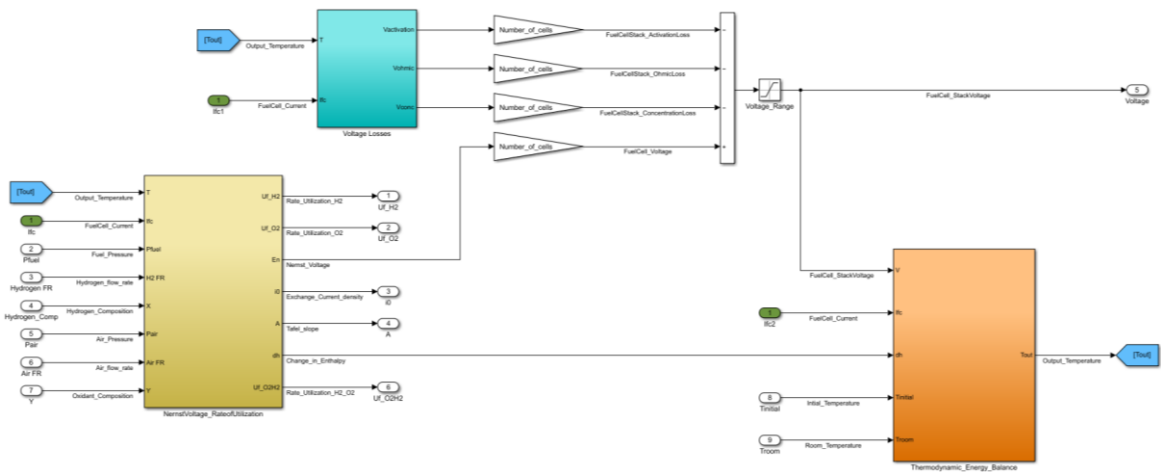

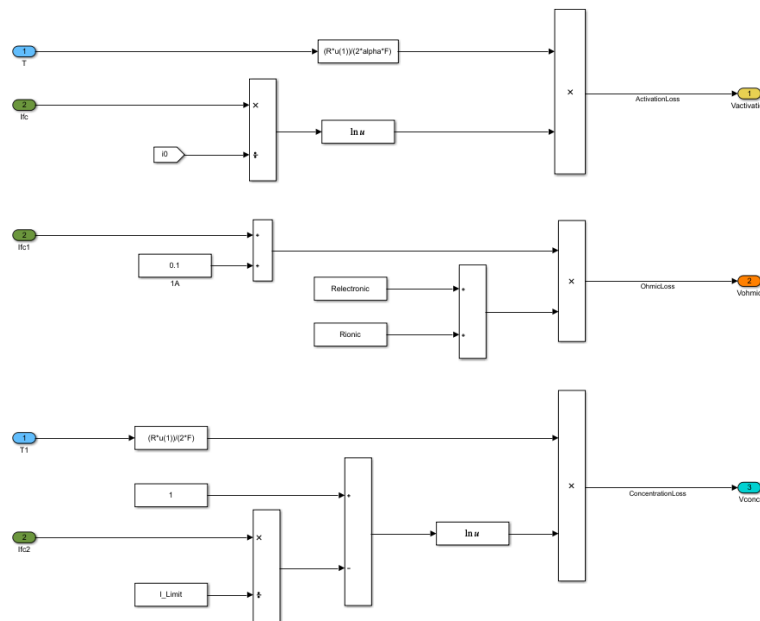Figure 3. Designed PEM type fuel cell
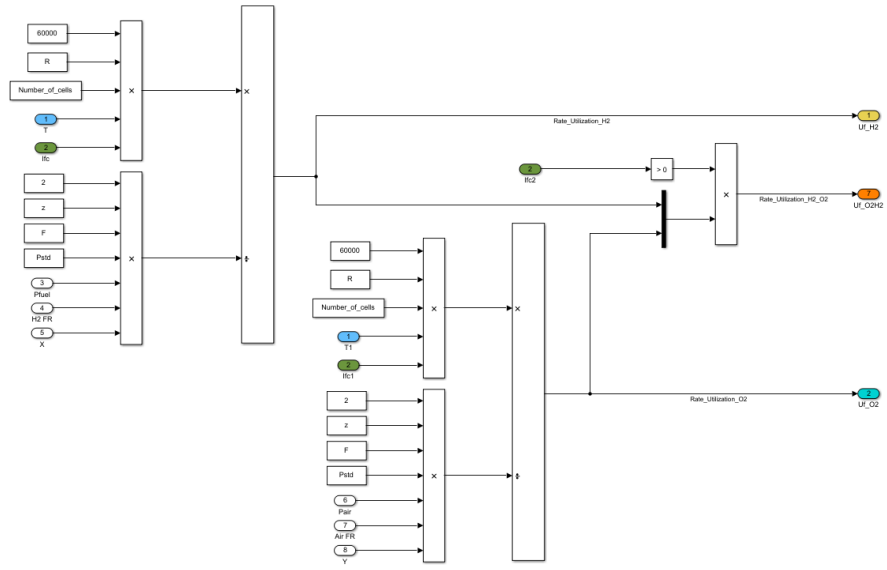

Figure 4. Subsystem voltage losses block
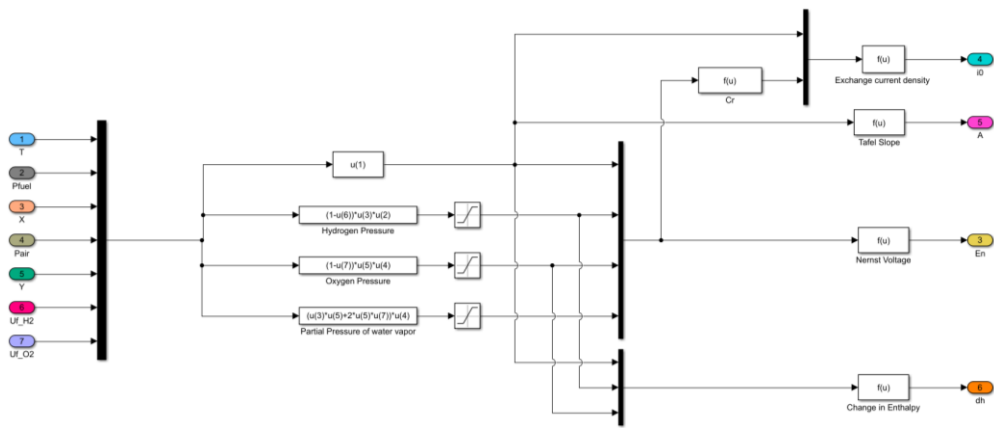
Figure 5. Subsystem rate of utilization block
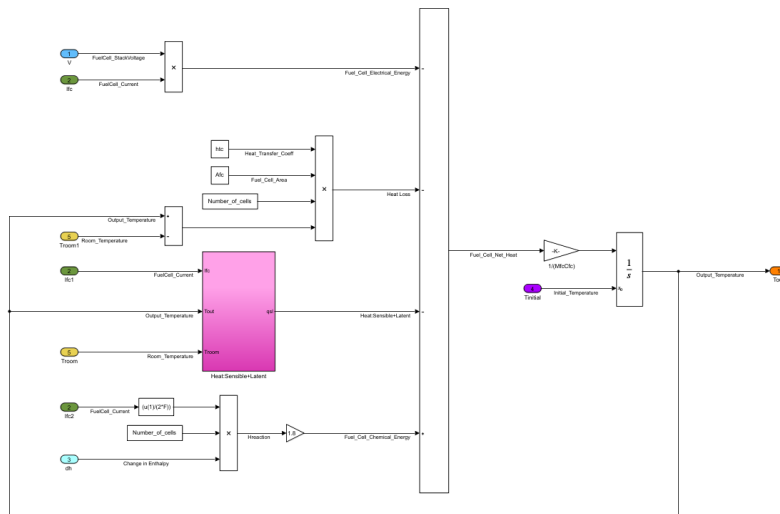

Figure 6. Subsystem Nernst voltage block

Figure 7. Subsystem thermodynamic energy balance

3. RESULTS AND DISCUSSION

3.1. Validation of designed PEM type fuel cell

The objective of the research is to carry out mathematical modelling of PEM type fuel cell for vehicle applications (4-wheeler) which further helps to test and get the idea of output power feasibility as per requirement. To design PEM type fuel cell, required parameters as mentioned in earlier sections are decided as: i) The fuel cell must produce 100 kW of power; ii) The fuel cell's operating temperature range is 0 to 100 °C; iii) The cathode and anode sides are under 3 atmospheres of pressure, or 303,975 Pascals (Pa); and iv) Number of cells calculated by using in (6) are 400. Based on the previously mentioned parameters and the equations presented in the earlier sections, a MATLAB/Simulink mathematical model of a PEM-type fuel cell is built following the methodology described.

Similar to the V-I characteristics shown in Figure 2, Figure 8 shows the voltage-current (V-I) characteristics of the PEM-type fuel cell. Using a MATLAB/Simulink software-available representative fuel cell vehicle example, the PEM-type fuel cell is tested and validated [16], [17]. The PEM-type fuel cell has a maximum power demand of 100 kW, and the maximum power output, according to the data, is also 100 kW. With a decreasing voltage as the current increases, the PEM-type fuel cell's performance closely resembles the fuel cell's theoretical behavior. The voltage of the fuel cell operates in three different regions: concentration, ohmic, and activation. The induced voltage in the PEM-type fuel cell that has been designed ranges from 481.2 to roughly 390 volts during the activation phase. The slow chemical reaction within the activation region causes a voltage reduction, resulting in a non-linear voltage drop.

Immediately after the activation region ends, the fuel cell begins to function in the ohmic region. This voltage ranges from about 390 volts at the beginning to about 315 volts at the end. Electrical resistance in the electrode causes ohmic loss within this ohmic region, which results in a linear voltage drop. It's important to note that this area, which corresponds to the point of maximum performance at 210 amperes and 340 volts, is thought to be ideal for fuel cell operation. The fuel cell then moves from the ohmic region to the mass transport region, which begins at about 310 volts and lasts until the cycle ends, when it approaches 290 volts. Diffusion of reactants from the flow channels to the reaction sites causes mass concentration loss in the mass transport region. Because reactants are transported to the reaction sites more slowly in higher-current operating zones, this loss is more noticeable.
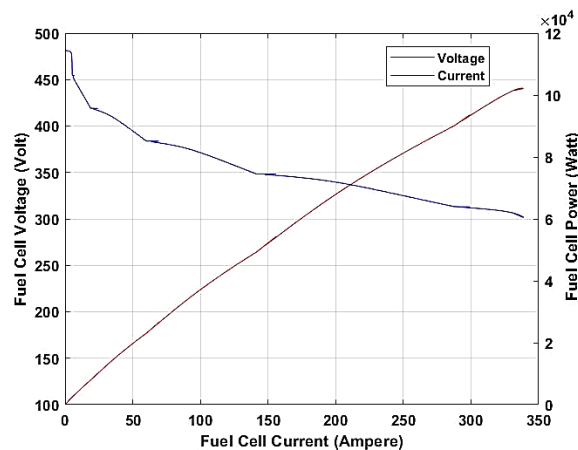

Figure 8. Simulated VI characteristics of the designed PEM type fuel cell

3.2. Performance test of designed PEM type fuel cell using NEDC

The performance test of the designed PEM-type fuel cell is done with the help of 'New European Driving Cycle' (NEDC) [18]. The NEDC is given as input to one of the examples of fuel cell vehicles available in MATLAB/Simulink software. NEDC provides different test points at different speeds, and the power requirement and performance test of the vehicle for different real-time test conditions are observed.

The NEDC cycle runs for 1160 seconds. The output voltage, output current, efficiency, temperature, and output power performance of the designed PEM-type fuel cell are observed. During performance testing, the output voltage and current behavior [19] of the designed PEM-type fuel cell follow those of the theoretical fuel cell. As the speed of the vehicle increases, the current demand increases, and as the current increases, the fuel cell's voltage decreases. After 800 seconds, the vehicle's speed increased, and further speed increased to 120 kmph, as illustrated in Figure 9. The output current of the designed PEM-type fuel cell, as illustrated in

Figure 10(a), is increasing, and in that period, the output voltage, as shown in Figure 10(b), is decreasing to satisfy the power requirement of the vehicle through the motor of the vehicle.

The fuel cell's irreversible efficiency is in the range of 40 to 60% [20]. The efficiency of the designed PEM-type fuel cell can be observed in Figure 11(a). By ignoring the lowest and highest peaks, the mean efficiency of a PEM-type fuel cell, as observed in Figure 11(a), is also in the range of 45 to 60%. The fuel cell's temperature operating range is from 25 to 100, i.e., 298 K to 373 K. As observed from Figure 11(b), the range of temperatures within which the designed PEM-type fuel cell is operating is also 298 to 373 K, which is near the stated operating temperature range of the fuel cell.

The vehicle's electric motor efficiently supplies the required power depending on a number of variables, including speed and load. The vehicle's battery and fuel cell power work together to meet these power needs. The PEM-type fuel cell intended for the NEDC cycle is tested, and its performance is assessed under a range of real-time test conditions in Figure 12. The designed PEM-type fuel cell and the vehicle's battery work together to guarantee that the electric motor's power needs are sufficiently satisfied. As observed from Figure 12, the motor power requirement of the motor is up to 25 kW, supplied by the designed PEM type fuel cell, and the remaining power of the designed PEM type fuel cell is used for regenerative braking, i.e., for the charging of the battery when it is not supplying power. The motor power requirement at high speed is from 1000 seconds to 1160 seconds, i.e., from 30 kW to about 70 kW. Thus, when the designed PEM-type fuel cell alone cannot fulfill the power requirement of the motor, the remaining power requirement of the motor is supplied by the battery of the vehicle, which is charged during regeneration mode. In this way, the validation of the designed PEM-type fuel cell is done using NEDC.
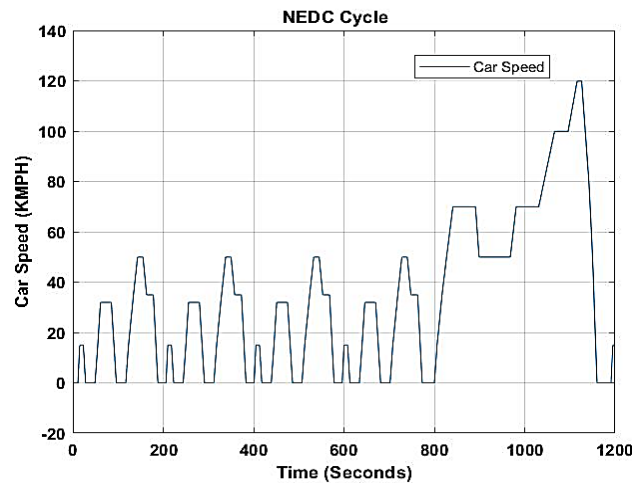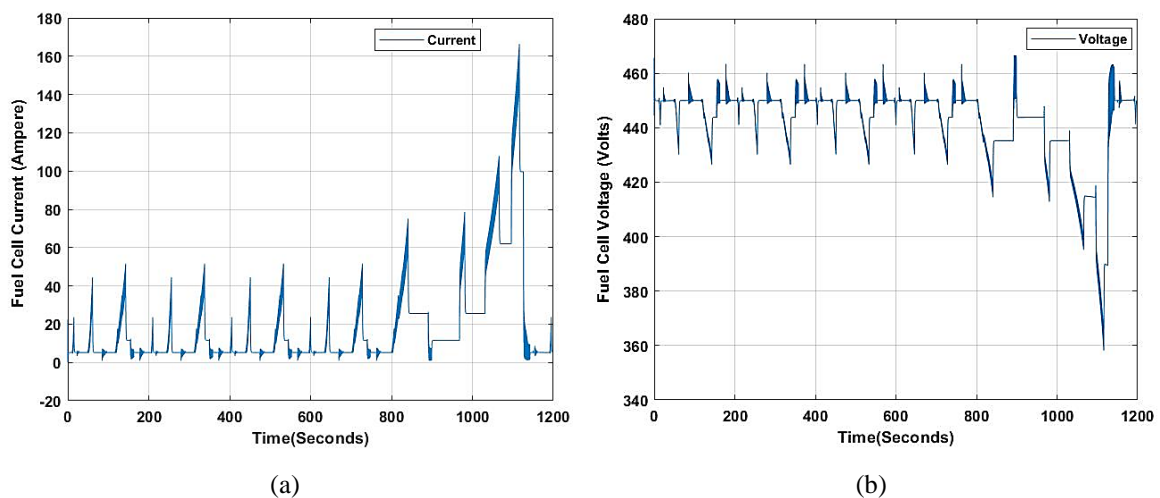

Figure 9. New European driving cycle (NEDC)

(a)   (b)

Figure 10. Performance of designed PEM type fuel cell (a) output current and (b) output voltage

(a)   (b)
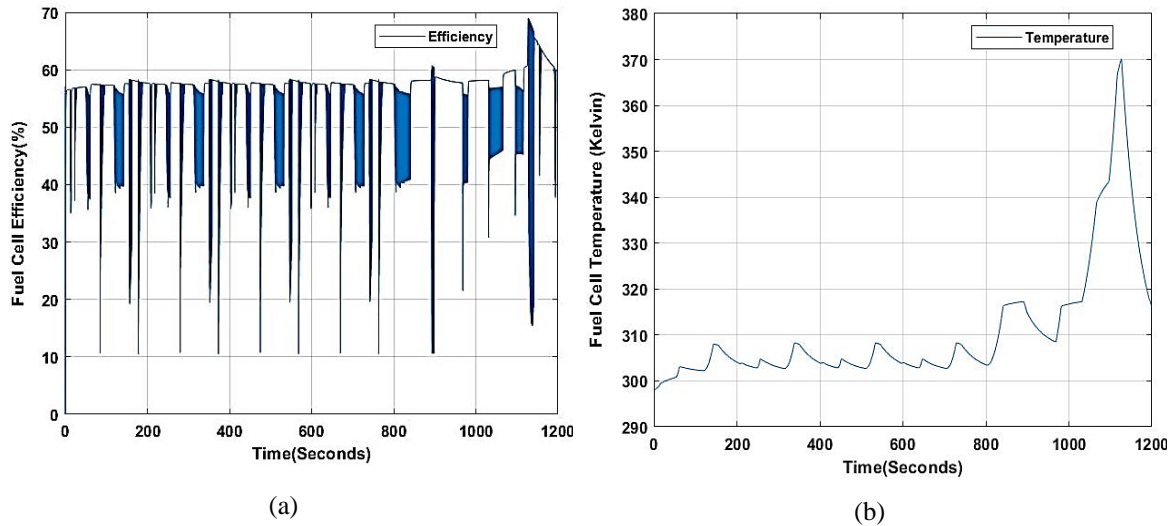
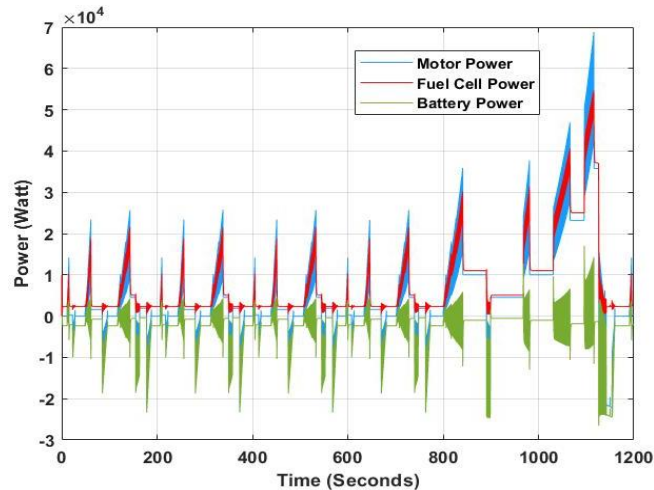Figure 11. Designed PEM type fuel cell, (a) efficiency and (b) temperature

Figure 12. Output power at different load and speed conditions by designed PEM fuel cell and
battery for motor

Fuel cell modeling can be done by considering the double-layer charge effect [21]. In the double-layer charging effect, at the junction point where the porous cathode meets the membrane, two polar, oppositely charged layers are formed. These are electrochemical double layers [4], [22]. The fuel cell model incorporates the double-layer charged effect by calculating output voltage using concentration voltage drop [23].

When the frequencies are higher, the impedance in a fuel cell acts like a resistance with an inductance that is connected in series. Because the double-layer capacitor filters current harmonics at these frequencies, they have negligible influence in regard to the reactions that are chemical in nature [24], [25]. The lifetime of a PEM-type fuel cell is influenced by low-frequency current ripple, which must be controlled within a certain minimum range. To control the low-frequency current ripple, several control methods, such as current mode control and current mode control with a notch filter in the voltage loop, are necessary [26], [27]. As the scope of this research is limited to the modeling of the PEM-type fuel cell, further work can be done to reduce low-frequency current ripple by implementing various control methods.

4.   CONCLUSION

Mathematical modeling of PEM-type fuel cells is done for vehicle applications (4-wheelers). Fuel cell models are available in MATLAB and Simulink, and by using these examples, this PEM-type fuel cell model is validated. The results drawn from the designed PEM-type fuel cell model are as follows: i) This model of a

PEM-type fuel cell has the same V-I (voltage-current) characteristics as the PEM-type fuel cell that is thought to work in theory; ii) A PEM-type fuel cell meets the maximum power requirement. Furthermore, at various load conditions, the proposed PEM-type fuel cell's power output is in accordance with the vehicle's power requirements; iii) The best operating region for PEM-type fuel cells is the ohmic range, where PEM-type fuel cells operate within their optimum range with better efficiency; iv) NEDC was used to test the behavior of the designed PEM-type fuel cell. The stack properties observed are comparable to those achieved in prior investigations. The behavioral statistics related to energy consumption are the same as those from earlier studies; v) The designed PEM-type fuel cell's efficiency is between 45% and about 60%; vi) The temperature of the designed PEM-type fuel cell is within the range of 25 to 100, which is as per the acceptable requirement for functioning.

REFERENCES

[1]   J. J. Baschuk and X. Li, "A general formulation for a mathematical PEM fuel cell model," *J. Power Sources*, vol. 142, no. 1–2, pp. 134–153, Mar. 2005, doi: 10.1016/j.jpowsour.2004.09.027.
[2]   H. Sadek, R. Chedid, and D. Fares, "Power sources sizing for a fuel cell hybrid vehicle," *Energy Storage*, vol. 2, no. 2, Apr. 2020, doi: 10.1002/est2.124.
[3]   D. B. Lata, A. Ahmad, O. Prakash, M. M. Khan, R. Chatterjee, and S. M. M. Hasnain, "Impact of Exhaust Gas Recirculation (EGR) on the Emission of the Dual-Fuel Diesel Engine with Hydrogen as a Secondary Fuel," *J. Inst. Eng. Ser. C*, vol. 102, no. 6, pp. 1489–1502, Dec. 2021, doi: 10.1007/s40032-021-00776-7.
[4]   A. L. Dicks and D. A. J. Rand, *Fuel Cell Systems Explained*. 2018. doi: 10.1002/9781118706992.
[5]   Y. Manoharan *et al.*, "Hydrogen Fuel Cell Vehicles, Current Status, and Future Prospect," *Appl. Sci.*, vol. 9, no. 11, p. 2296, Jun. 2019, doi: 10.3390/app9112296.
[6]   D. Sarma, P. B. Barua, N. Dey, S. Nath, M. Thakuria, and S. Mallick, "Investigation and Taguchi Optimization of Microbial Fuel Cell Salt Bridge Dimensional Parameters," *J. Inst. Eng. Ser. C*, vol. 100, no. 1, pp. 103–112, Feb. 2019, doi: 10.1007/s40032-017-0436-0.
[7]   C. Spiegel, *PEM Fuel Cell Modeling and Simulation Using Matlab*. Elsevier, 2008. doi: 10.1016/B978-0-12-374259-9.X5001-0.
[8]   E. Chan, F. Dawson, H. Bekker, and E. Livshits, "A software simulation program for a hybrid fuel cell - battery power supply for an electric forklift," in *2007 European Conference on Power Electronics and Applications*, IEEE, 2007, pp. 1–10. doi: 10.1109/EPE.2007.4417368.
[9]   A. Kirubakaran, S. Jain, and R. K. Nema, "The PEM Fuel Cell System with DC/DC Boost Converter: Design, Modeling and Simulation," *Int. J. Recent Trends Eng.*, vol. 1, no. 1, pp. 157–161, 2009.
[10] R. O'Hayre, S. Cha, W. Colella, and F. B. Prinz, *Fuel Cell Fundamentals*. Wiley, 2016. doi: 10.1002/9781119191766.
[11] W. Chanpeng and Y. Khunatorn, "The effect of the input load current changed to a 1.2 kW PEMFC performance," *Energy Procedia*, vol. 9, pp. 316–325, 2011, doi: 10.1016/j.egypro.2011.09.034.
[12] S. Haji, "Analytical modeling of PEM fuel cell i–V curve," *Renew. Energy*, vol. 36, no. 2, pp. 451–458, Feb. 2011, doi: 10.1016/j.renene.2010.07.007.
[13] I. P. Sahu, G. Krishna, M. Biswas, and M. K. Das, "Performance Study of PEM Fuel Cell under Different Loading Conditions," *Energy Procedia*, vol. 54, pp. 468–478, 2014, doi: 10.1016/j.egypro.2014.07.289.
[14] R. L. Edwards and A. Demuren, "Interface model of PEM fuel cell membrane steady-state behavior," *Int. J. Energy Environ. Eng.*, vol. 10, no. 1, pp. 85–106, Mar. 2019, doi: 10.1007/s40095-018-0288-2.
[15] M. H. Nehrir and C. Wang, "Modeling and Control of Fuel Cells," in *IEEE Press Series on Power Engineering*, Wiley-IEEE Press, 2009. doi: 10.1109/9780470443569.
[16] J. Yan, C. Zhou, Z. Rong, H. Wang, H. Li, and X. Hu, "Simulation of the Dynamic Characteristics of a PEMFC System in Fluctuating Operating Conditions," *Energies*, vol. 13, no. 14, p. 3596, Jul. 2020, doi: 10.3390/en13143596.
[17] J. B. Benziger, M. B. Satterfield, W. H. J. Hogarth, J. P. Nehlsen, and I. G. Kevrekidis, "The power performance curve for engineering analysis of fuel cells," *J. Power Sources*, vol. 155, no. 2, pp. 272–285, Apr. 2006, doi: 10.1016/j.jpowsour.2005.05.049.
[18] S. Zhou, J. Jin, and Y. Wei, "A Driving Cycle for a Fuel Cell Logistics Vehicle on a Fixed Route: Case of the Guangdong Province," *World Electr. Veh. J.*, vol. 12, no. 1, p. 5, Jan. 2021, doi: 10.3390/wevj12010005.
[19] M. A. Salam *et al.*, "Effect of Temperature on the Performance Factors and Durability of Proton Exchange Membrane of Hydrogen Fuel Cell: A Narrative Review," *Mater. Sci. Res. India*, vol. 17, no. 2, pp. 179–191, Sep. 2020, doi: 10.13005/msri/170210.
[20] U. S. D. of Energy, "Comparison of Fuel Cell Technologies," 2016. [Online]. Available: https://www.energy.gov/eere/fuelcells/articles/comparison-fuel-cell-technologies-fact-sheet
[21] S. V. Puranik, A. Keyhani, and F. Khorrami, "State-Space Modeling of Proton Exchange Membrane Fuel Cell," *IEEE Trans. Energy Convers.*, vol. 25, no. 3, pp. 804–813, Sep. 2010, doi: 10.1109/TEC.2010.2047725.
[22] A. Schneuwly, M. Bärtschi, V. Hermann, G. Sartorelli, R. Gallay, and R. Koetz, "BOOSTCAP Double-Layer Capacitors for Peak Power Automotive Applications," in *Montena*, 2006, p. 1.
[23] A. E.-M. A. Mokarrab, A. M. Azmy, and S. A. Mahmoud, "Effect of process parameters on the dynamic behavior of polymer electrolyte membrane fuel cells for electric vehicle applications," *Ain Shams Eng. J.*, vol. 5, no. 1, pp. 75–84, Mar. 2014, doi: 10.1016/j.asej.2013.05.001.
[24] L. Zhang and X. Ruan, "Control Schemes for Reducing Second Harmonic Current in Two-Stage Single-Phase Converter: An Overview From DC-Bus Port-Impedance Characteristics," *IEEE Trans. Power Electron.*, vol. 34, no. 10, pp. 10341–10358, Oct. 2019, doi: 10.1109/TPEL.2019.2894647.
[25] G. Fontes, C. Turpin, S. Astier, and T. A. Meynard, "Interactions Between Fuel Cells and Power Converters: Influence of Current Harmonics on a Fuel Cell Stack," *IEEE Trans. Power Electron.*, vol. 22, no. 2, pp. 670–678, Mar. 2007, doi: 10.1109/TPEL.2006.890008.
[26] H. Deng, Q. Li, Z. Liu, L. Li, and W. Chen, "Low Frequency Current Ripple Mitigation of Two Stage Three-Phase PEMFC Generation Systems," *J. Power Electron.*, vol. 16, no. 6, pp. 2243–2257, Nov. 2016, doi: 10.6113/JPE.2016.16.6.2243.
[27] M. Huang *et al.*, "Research on hybrid ratio of fuel cell hybrid vehicle based on ADVISOR," *Int. J. Hydrogen Energy*, vol. 41, no. 36, pp. 16282–16286, Sep. 2016, doi: 10.1016/j.ijhydene.2016.05.130.

BIOGRAPHIES OF AUTHORS

Ankush Babaji Aher 🆔 🇬 sc ◐ received Bachelor of Engineering (B.E.) degree in Mechanical Engineering from the Savitribai Phule Pune University (SPPU), India and Master of Technology (M.Tech.) degree in Mechatronics from College of Engineering, Pune (COEP), Maharashtra, India in 2021. He carried out his research work in the field of fuel cell at Automotive Research Association of India (ARAI), Pune, Maharashtra, India. He is currently working as Model Based System Engineer at L&T Technology Services Limited, Vadodara, Gujarat, India. His main research interests include renewable energy, fuel cell systems, fuel cell technology, system modelling and simulation using model-based design (MBD), Stateflow, and Simulink in MATLAB. He can be contacted at email: ankushaher20@gmail.com or aherab19.prod@coep.ac.in.

Sudhir Madhav Patil 🆔 🇬 sc ◐ received Bachelor of Engineering degree in Mechanical Engineering from the North Maharashtra University, Maharashtra, India and Master's and Ph.D. degree in Production Engineering from the Savitribai Phule Pune University (SPPU), Maharashtra, India. He is a Member of The Institution of Engineers (India) and a Life Member of Tribology Society of India (LMTSI). His main research interest includes mechatronics, manufacturing automation, robotics and AI, and Tribology. He has published several research papers and is a co-inventor for couple of Indian patents. He can be contacted at email: smp.prod@coeptech.ac.in, sudhir.smp@gmail.com, or smp.mfg@coeptech.ac.in.

Tole Sutikno 🆔 🇬 sc ◐ is a lecturer and the head of the Master Program of Electrical Engineering at the Faculty of Industrial Technology at Universitas Ahmad Dahlan (UAD) in Yogyakarta, Indonesia. He graduated from Universitas Diponegoro with a Bachelor of Engineering in 1999, Universitas Gadjah Mada with a Master of Engineering in 2004, and Universiti Teknologi Malaysia with a Doctor of Philosophy in Electrical Engineering in 2016. Electrical engineering comprises each of the three degrees. He has been a Professor at UAD in Yogyakarta, Indonesia, since July 2023, after serving as an Associate Professor from June 2008. He is the current Editor-in-Chief of TELKOMNIKA and the head of the Embedded Systems and Power Electronics Research Group (ESPERG). According to Stanford University and Elsevier BV's list of the most prominent scientists from 2021 to the present, he ranks among the top 2% of researchers globally. His research interests include digital design, industrial applications, electronics, informatics, power electronics, motor drives, renewable energy, FPGA applications, embedded systems, artificial intelligence, intelligent control, digital libraries, and information technology. He can be contacted at email: tole@te.uad.ac.id.